

BM-MSCs-derived ECM modifies multiple myeloma phenotype and drug response in a source-dependent manner

AMJD IBRAHEEM, OSHRAT ATTAR-SCHNEIDER, MAHMOUD DABBAH, OSNAT DOLBERG JARCHOWSKY, SHELLY TARTAKOVER MATALON, MICHAEL LISHNER¹, and LIAT DRUCKER¹

KFAR SABA, AND TEL AVIV, ISRAEL

Multiple myeloma (MM) malignant plasma cells accumulate in the bone marrow (BM) where their interaction with the microenvironment promotes disease progression and drug resistance. Previously, we have shown that MM cells cocultured with BM-mesenchymal stem cells (MSCs) modulated cells' phenotype in a MAPKs/translation initiation (TI)-dependent manner. Dissection of the coculture model showed that BM-MSCs secretomes and microvesicles (MVs) participate in this cross-talk. Here, we addressed the role of the BM-MSCs extracellular matrix (ECM).

MM cell lines cultured on decellularized ECM of normal donors' (ND) or MM patients' BM-MSCs were assayed for phenotype (viability, cell count, death, proliferation, migration, and invasion), microRNAs (MIR125a-3p, MIR199a-3p) and targets, MAPKs, TI epithelial-to-mesenchymal transition (EMT), CXCR4, and autophagy. Drug (doxorubicin, velcade) response of MM cells cultured on ND/MM-MSCs' ECM with/without adhered MVs was also evaluated.

ECM evoked opposite responses according to its origin: MM cells cultured on ND-MSCs' ECM demonstrated a rapid and continued decrease in MAPK/TI activation ($\downarrow 10\%–25\%$, $P < 0.05$) (15–24 hours) followed by diminished viability, cell count, proliferation, migration, and invasion (16–72 hours) ($\downarrow 10\%–50\%$, $P < 0.05$). In contrast, MM cells cultured on MM-MSCs' ECM displayed activated MAPK/TI, proliferation, EMT, and CXCR4 ($\uparrow 15\%–250\%$, $P < 0.05$). Corresponding changes in microRNAs relevant to the MM cells' altered phenotype were also determined. The hierarchy and interdependence of MAPKs/TI/autophagy/phenotype cascade were demonstrated. Finally, we showed that the ECM cooperates with MVs to modulate MM cells drug response.

These data demonstrate the contribution of BM-MSCs' ECM to MM niche design and underscore the clinical potential of identifying targetable signals. (Translational Research 2019; 000:1–13)

¹These authors contributed equally to this work.

From the Oncogenetic Laboratory, Meir Medical Center, Kfar Saba, Israel; Lung Cancer Research Laboratory, Meir Medical Center, Kfar Saba, Israel; Hematology Clinique, Meir Medical Center, Kfar Saba, Israel; Gastroenterology Laboratory, Meir Medical Center, Kfar Saba, Israel; Research Authority, Meir Medical Center, Kfar Saba, Israel; Sackler Faculty of Medicine, Tel Aviv University, Tel Aviv, Israel.

Submitted for Publication September 1, 2018; received submitted December 17, 2018; accepted for publication January 14, 2019.

Reprint requests: Liat Drucker, Oncogenetic Laboratory, Meir Medical Center, Tshernichovski st., Kfar Saba 44281, Israel. E-mail address: druckerl@clalit.org.il.

1931-5244/\$ - see front matter

© 2019 Elsevier Inc. All rights reserved.

<https://doi.org/10.1016/j.trsl.2019.01.003>

AT A GLANCE COMMENTARY

Ibraheem A, et al.

Background

This study demonstrates the contribution of bone marrow mesenchymal stem cells (BM-MSCs) extracellular matrix (ECM) to multiple myeloma (MM) niche design, disease progression, and drug response.

Translational Significance

We show that MM-MSCs' ECM promotes MM cells' MAPKs/translation initiation-dependent proliferation and migration, whereas normal donors (ND)-MSCs' ECM causes the opposite effect. We also demonstrate the cooperation of the BM-MSCs' ECM with BM-MSCs-derived microvesicles and its contribution to the MM cells response to doxorubicin and velcade.

BACKGROUND

The extracellular matrix (ECM) was initially regarded as an inert mechanical scaffold for cells.¹ This erroneous perception was amended with the increasing evidence of the ECM's active involvement in cell signaling and phenotypic design.¹

The ECM is a composite of proteins, collagens, proteoglycans, and glycosaminoglycans that assemble into a 3D structure that serves as a binding interface for multiple proteins.² This scaffold is dynamic in structure, rigidity, and composition and is continuously altered by cell secretion, various modifying enzymes, incorporation, and extraction of multiple growth factors, extracellular vesicles, and more.^{3,4} The constant change in ECM creates an information-rich signaling platform that is also niche specific in its composition and functions as an active component of healthy and pathologic microenvironments, cancer included.^{4,5}

It is well recognized that ECMs in tumor niches facilitate the cancer cells' survival, proliferation, and metastasis.^{6,7} Multiple studies have demonstrated that the bone marrow (BM) ECM is altered by the presence of tumor cells (metastatic or primary).^{5,8} Multiple myeloma (MM) malignant plasma cells accumulate and spread in the BM causing changes in this niche and subverting it into a cancer supporting microenvironment.^{2,9,10} Specifically, evidence shows that this interaction promotes disease progression via elevated proliferation, migration and most importantly cell-adhesion-mediated-drug resistance (CAM-DR).¹¹ As a result, the communications of the MM cells with their

BM microenvironment, particularly CAM-DR, are recognized as major obstacles to disease therapy.¹¹ Much progress in MM treatment has arisen from targeting the MM BM immune microenvironment¹² yet, less has progressed in the understanding of MM cells interaction with the nonhematopoietic cells residing in the BM niche such as the plastic mesenchymal stem cells (MSCs). Being multipotent, the MSCs are responsible for replenishing the niche stroma and contributing to its design.⁸

In the past several years, we have demonstrated that the MM cells maintain a highly significant dialogue with the BM-resident MSCs.¹³⁻¹⁷ We have shown that there are distinct differences between the crosstalk of MM cells with BM-MSCs from normal donors (ND-MSCs) and MM patients (MM-MSCs).^{14,16,17} The MM-MSCs promote the proliferation, survival, migration, invasion, and drug resistance of adjacent MM cells, whereas the ND-MSCs inhibit these traits. We have also shown that these phenotypical changes are mediated in a MAPKs/translation initiation (TI)-dependent manner.^{14,16,17} In order to identify the participants in this dynamic crosstalk, we dissected our coculture research model into several compartments.¹⁶ With this approach, we have identified the involvement of secreted components in this dialogue¹⁶ including microvesicles (MVs).¹⁴

In the present study, we aimed to characterize the involvement of the BM-MSCs' secreted ECM in MM cells' phenotypic design. Particular attention was attributed to differences between the effect of ND-MSCs' ECM effects and those of the MM-MSCs' ECM. We used a 2D culture model that allowed us to assess multiple primary BM-MSCs ECM samples in a reproducible and reliable manner. Indeed, we observed unequivocal differences between the influences of BM-MSCs ECMs in accordance to their normal or pathologic source and uncovered another layer in the malignant conversion of the BM niche "bystanders" into active MM promoters. We also addressed the role of MVs attached to the ECM in promoting CAM-DR.

MATERIALS AND METHODS

Cell lines. Authenticated MM cell lines U266, MM1S, RPMI-8226, and ARP-1 were cultured with RPMI 1640 supplemented with 10% heat-inactivated fetal bovine serum (FBS), antibiotics, and glutamine (Biological Industries).

BM-MSCs isolation and propagation. BM samples were obtained from femur head BM samples of normal donors (ND), undergoing elective full hip replacement surgery for hip osteoarthritis, and femoral neck fracture

Table 1. Multiple Myeloma patients' clinical characteristics

Patient number	Gender	Age	Plasma cells in BM aspirate mononuclear cells (%)	Isotype (g/dL)	Free light chain	B2 microglobulin	Albumin	ISS
N1	F	53	30	Hypo γ	κ 3100	9.1	3.5	3
N2	F	80	10	IgG 3.13	λ 195	4.9	3.1	2
N3	M	56	40	IgG 2.16	λ 283	N/A	4	N/A
N4	M	78	25	Hypo γ	κ 1500	3.6	4.4	2
N5	M	77	75	IgA 2.02	κ 43	N/A	3	N/A
N6	F	85	15	IgA 1.1	κ 64	3.5	3.6	2
N7	M	79	50	Hypo γ	κ 4020	6.3	3.9	3
N8	F	68	90	IgG 6.88	λ 214	6.5	3.4	3
N9	M	60	15	IgA 2.16	λ 375	3.6	3.9	2
N10	M	84	80	IgG 6.3	κ 60	6.8	3.5	3
N11	F	67	90	Hypo γ	λ 2900	7.7	4.1	3
N12	F	88	50	IgG 6.22	κ 60	5.6	3.1	3
N13	M	77	70	Hypo γ	κ 2300	N/A	4.1	N/A
N14	F	53	70	N/A	κ 2160	N/A	3.5	N/A
N15	F	78	25	IgG 4.57	κ 2490	33.7	3.4	3
N16	M	82	20	IgG 2.14	κ 497	4.8	3.7	2
N17	M	83	20	Hypo γ	λ 133	3.4	4.5	1
N18	F	90	50	IgG 6.97	λ 480	9.7	2.3	3
N19	M	69	80	IgG 3.08	κ 267	7.5	3.7	3
N20	M	61	25	IgA 2.47	λ 4550	3.7	3.7	2
N21	M	92	75	IgA 6.05	κ 40	14.1	2	3

(n = 50), and MM patients' BM aspirates taken for medical purposes (Table 1; n = 21) at Meir Medical Center. All participants signed informed consent forms approved by Meir Medical Center Helsinki Committee. MSCs were isolated, propagated, characterized, and differentiated as described by us previously.¹³⁻¹⁶

Microvesicles isolation and application to MM cell lines. Microvesicles (MVs) were isolated from conditioned media collected from 80% confluent BM-MSCs cultures (2–6 weeks).¹⁸ Briefly, media was obtained after cell removal by centrifugation at 800 X g for 5 minutes and then centrifuged at 4500 X g for 5 minutes to discard large debris. After centrifugation twice at 20,000 X g (Beckman Ti70 rotor; Beckman Coulter) for 60 minutes at 4°C, the MVs were washed and resuspended in PBS. Collected MVs were characterized and validated (Microscopy and FACS) as previously.^{14,16}

MM cell lines' exposure to BM-MSCs' ECM. Bonafide MSCs (ND and MM) were seeded 75,000 cells/24 well in RPMI 1640 supplemented with antibiotics and 10% FBS for 72 hours. After 72 hours, we removed the BM-MSCs (decellularization) using double distilled water (DDW) and NH⁴OH and left the secreted ECM embedded on the plastic intact (Fig 1). Next, we seeded MM cells (100,000 cells/24 well) (MM1S, U266, RPMI 8226, and ARP-1) on the BM-MSCs' ECM for different time spans (1.5, 4, 24, 48, and 72 hours) after which the cells were harvested and assayed for phenotype and signaling. MM cell lines cultured on their own

respective 72 hours ECM served as experimental controls. The response of the MM cells (phenotype, signaling) were recorded and analyzed as described in the statistics section.

Trypan blue. Total, viable and dead cell counts were assayed by trypan blue dye. Cells were automatically counted by Countess (Invitrogen).¹⁵

Immunocytochemistry. MSCs (50,000) were cyto-spinned (Labofuge, 400R), fixed (4% paraformaldehyde, 100% methanol), blocked (5.5% goat serum), and incubated with primary antibodies for Vimentin or Keratin overnight at 4°C. Cells were visualized with a BX41 microscope (40 \times) (Olympus); images were taken with DP70 digital camera and DP Controller software (Olympus). Validation of ECM components post decellularization was done by staining collagen with Aniline Acid stain (2.5 g aniline blue in 2 mL glacial acetic acid and 100 mL DDW-30') and elastin with orcein acid stain (1 g orcein in 100 mL 70% EtOH and 1 mL 25% HCl-48 hours) and microscopic analysis.

Cell viability assay. Cell viability was assayed with cell proliferation reagent WST-1 (Roche, Basel, Switzerland) as described before.^{15,18}

Western blotting. Cells were lysed in lysis buffer; protein levels were determined by BCA assay as done previously. Proteins lysates were immunoblotted as we described previously^{15,18} using rabbit/mouse antihuman: p-eIF4E (Ser-209)/total eIF4E, p-eIF4GI(Ser-1108)/total eIF4GI, p4EBP(Ser-65)/total 4EBP, p-mTOR(Ser-2448)/

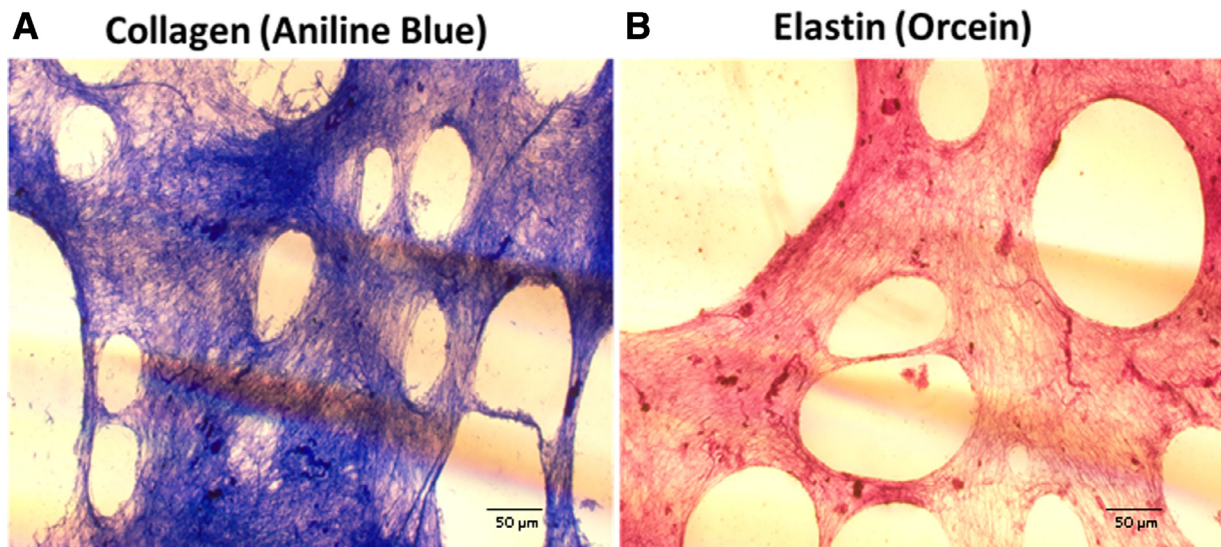


Fig 1. Validation of ECM integrity after decellularization. BM-MSCs were seeded in 24 wells, 72 hours later cells were decellularized using DDW and strong base (NH₄OH-1:1000) leaving the ECM in the wells. ECM was stained for the highly expressed collagen with aniline blue (A) and the less abundant elastin with orcein (B). Their presence indicates that the remnant ECM is intact and appropriate for our study.

total mTOR, Beclin-1 (Cell Signaling Technology, Danvers, MA), p-MNK (Thr-197/Thr-202)/total MNK, SMAD5 (Epitomics, Burlingame, CA); NFκB, c-Myc, HIF1α, PCNA (Santa-Cruz, CA) Cyclin D1, pERK1/2, pJNK, total ERK1/2 and total JNK (Cell Signaling Technology, Danvers, MA); LC3-II, CXCR4 (Santa-Cruz, CA), Slug and Snail (Cell Signaling Technology, Danvers, MA), tubulin (Sigma).

qRT-PCR for microRNA. MicroRNA was extracted with TRI Reagent (Sigma) and was converted to cDNA using the Quanta reverse-transcription kit (Quantabio, Beverly, MA) according to manufacturer's instructions. Briefly, RNA was polyadenylated with ATP by poly(A) polymerase and reverse transcribed using poly (T) adapter primer. MicroRNAs were detected using a mature DNA sequence as the specific forward primer (5'–3') and a universal reverse primer (3'–5') provided in the Quanta reverse-transcription kit. Human, small, nucleolar RNA RNU44 was amplified as an internal control. Amplification was performed using Power SYBR Green PCR Master Mix (Quantabio).

Migration/transwell assay. A total of 100,000 MM cells were cultured in the upper chamber of transwell plate 8.0 μm (corning) with RPMI 3% FBS. The lower chamber contained Fibronectin (human plasma, Sigma, 20 μM,) dissolved in RPMI 10% FBS. Additionally, ECM from different sources (ND-MSCs, MM-MSCs, and MM cells as a control) were presented in the lower chamber, migrated cells present in the lower chamber were enumerated after 24 hours using the automatic Countess (Invitrogen).

Zymogram. Collected supernatants of treated cells were assayed for MMP9 and MMP2 gelatinase activity. Aliquots (25 μL) of the media were electrophoresed at nonreducing conditions in 10% polyacrylamide gels containing 1 mg/mL gelatin type A (Sigma). Gels were washed twice in 2.5% Triton X-100 for gelatinase renaturation and incubated overnight in 50 mM Tris-HCl (pH 7.5) and 5 mM CaCl₂. Coomassie blue staining followed by destaining allowed visualization of clear lysis zones against a blue background.

Inhibitors and drugs. 4EGI-1 (eIF4E/eIF4G Interaction Inhibitor) (35 μM, dissolved in DMSO). 3 methyladenine (3MA, autophagy inhibitor) (7.5 mM, dissolved in ddH₂O) (Sigma). MAPK inhibitors; SP600125 (20 μM, JNK inhibitor, Biomol Int.) and U0126 (10 μM, MEK1/2 inhibitor, CST, USA). Both inhibitors were dissolved in DMSO. Velcade (Bortezomib; CAS179324-69-7) and Doxorubicin (TEVA) were obtained from Meir Medical Center pharmacy and used at working concentrations of 1 nM and 0.5 μM, respectively.¹⁹⁻²¹

Statistical analysis. Student's paired/unpaired *t* tests were applied in the analyses of differences between cohorts of MM cells exposed to the different ECMs (not pooled). An effect was considered significant when *P* value is equal to or less than 0.05. All experiments were conducted at least 3 separate times. An additive effect was verified by drugs' interaction formula $q = \frac{P(A+B)}{P(A)+P(B)-P(A)*P(B)}$ [$q < 0.85$ —antagonist; $q > 1.15$ —synergist; $1.15 > q > 0.85$ —additive]. All experiments were conducted 3–7 separate times.

RESULTS

The phenotype of MM cell lines is affected by BM-MSCs ECM in a source-dependent manner. **Viability.** MM cell lines cultured for 72 hours on their own ECM (control), MM-MSCs' and ND-MSCs' ECMs were assayed for cell viability using the WST1 reagent. Significant yet opposing changes were recorded in MM cells' viability on both ND and MM-MSCs' ECMs compared to their viability when cultured on their own ECM (Fig 2, A). Specifically, ND-MSCs ECM reduced MM cell lines viability ($\downarrow 5\% - 15\%$, $P < 0.05$), whereas MM-MSCs ECM elevated MM cells' viability ($\uparrow 30\% - 60\%$, $P < 0.01$; Fig 2, A).

Proliferation and death. Based on the altered viability, we wanted to see whether this was attributed to changes in proliferation and/or death rates. Thus, we stained the MM cells exposed to respective cell lines' and BM-MSCs ECMs with trypan blue and enumerated live/dead/total cells. We registered increased live/total MM cells when exposed to MM-MSCs' ECM ($\uparrow 15\% - 25\%$, $P < 0.05$; Fig 2, B) with slightly decreased levels of dead cells (raw data) ($\downarrow 5\%$, $P < 0.05$; Fig 2, C). In contrast, there were decreased live/total MM cells when exposed to the ND-MSCs' ECM ($\downarrow 5\% - 30\%$, $P < 0.05$; Fig 2, B) and minutely higher levels of dead cells (raw Data) ($\uparrow 5\%$, $P < 0.05$; Fig 2, C). Cell death was further assessed by flow cytometry with similar results (data not shown). Taken together, these observations suggest that the elevation in total/live counts upon culture with MM-MSCs ECM is derived primarily from increased proliferation. For final validation of this conclusion, we assayed the expression levels

of the proliferation marker PCNA by immunoblotting (Fig 2, D and E). Indeed, results indicated that MM-MSCs ECM elevated PCNA levels in adjacent MM cell lines ($\uparrow 30\% - 60\%$, $P < 0.05$), whereas ND-MSCs ECM diminished PCNA levels ($\downarrow 10\% - 20\%$, $P < 0.05$) compared to experimental control (MM cells cultured on respective cell lines' ECM).

Autophagy. In previous studies, we have shown that BM-MSCs elevate autophagy in MM cell lines.¹⁶ Here, we wanted to explore the role of the BM-MSCs ECM in this phenomenon. Therefore, we assayed (immunoblotting) the levels of established autophagy markers in MM cell lines cultured for 72 hours on ND and MM-MSCs' ECMs. Results demonstrated that ND-MSCs' ECM and MM-MSCs' ECM increased autophagy markers LC3-II and Beclin (ND- $\uparrow 10\% - 20\%$, MM- $\uparrow 25\% - 50\%$, $P < 0.05$) but MM-MSCs' ECM did so to a greater extent ($P < 0.05$; Fig 2, E and F). In order to determine the importance of autophagy to MM cells' survival/proliferation, we re-enumerated ECM treated MM cells in the presence or absence of autophagy inhibitor 3MA. Importantly, since MM cells depend on autophagy for their normal survival and proliferation,¹⁶ its inhibition resulted in a background negative effect of decrease in live cells ($\downarrow 30\%$, $P < 0.05$). When we inhibited autophagy in MM cell lines cultured on MM-MSCs' ECM, the live cell counts were reduced to the control baseline levels as well ($\downarrow 45\%$, $P < 0.05$), thereby causing the background effect and cancelling the ECMs' contribution (Fig 2, G). These results attest to the indispensable role of autophagy in the MM-MSCs' ECM-induced MM cells' proliferation.

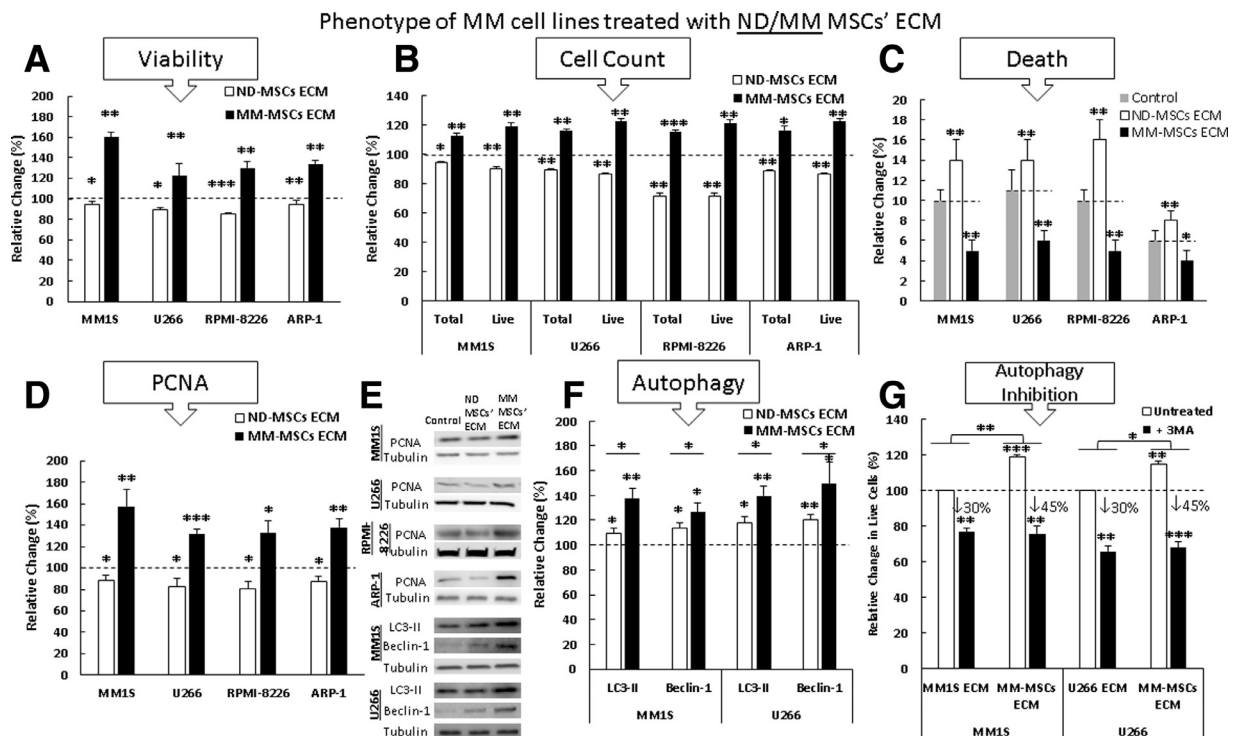


Fig 2. BM-MSCs' ECM effect on MM cell lines' phenotype. MM cell line cell lines (MM1S, U266, RPMI-8226, ARP-1) were cultured on BM-MSCs ECM (ND, MM, and its own for control). After 72 hours, the cells were harvested and assessed for changes in the cells' (A) viability (WST1), (B, C) proliferation and death (trypan blue). Next, cell lines were lysed and immunoblotted for PCNA proliferation marker (D, E). MM1S and U266 cells were also cultured for 24 hours on respective ECM, lysed, and immunoblotted for autophagy markers LC3II and Beclin (F) and cell count in the presence of autophagy inhibitor 3MA (G). Tubulin served as loading control. Results are expressed as percent (Mean \pm SE, $n \geq 4$) of respective change in control cells treated with its own ECM (dotted line). Asterisks depict statistical significance (* $P < 0.05$, ** $P < 0.01$, *** $P < 0.001$).

Migration and invasion. Next, we assayed the influence of the respective BM-MSCs' ECMs (ND, MM) on the MM cells' migratory and invasive capabilities by transwell assay (MM1S, U266, RPMI 8226, ARP-1) and MMPs' zymogram (MM1S, U266), respectively. An increase in cell migration ($\uparrow 30\%$ – 45% , $P < 0.05$) and MMPs 2 and 9 activities ($\uparrow 20\%$ – 50% , $P < 0.05$) were observed in MM cell lines cultured on MM-MSCs' ECM (24 hours and 72 hours, respectively; Fig 3, A and B). On the contrary, there was a decrease in the migration and MMPs activities of MM cells exposed to ND-MSCs' ECM ($\downarrow 10\%$ – 35% and $\downarrow 15\%$, respectively; $P < 0.05$; Fig 3, A and B). It is well established that the migratory phenotype of cancer cells is often associated with a phenotypical change and increased expression of mesenchymal markers. Thus, we assayed EMT (epithelial to mesenchymal) markers (slug and Snail) 24 hours after the exposure to ECM. An increased expression was registered upon exposure of the MM cell lines to BM-MSCs' ECM (ND, MM) yet the elevation was significantly greater in the cells exposed to MM-MSCs' ECM ($\uparrow 100\%$, $P < 0.05$; Fig 3, C).

The role of CXCR4 in cancer cell metastasis is also well recognized²² and its elevation in MM cells cocultured with MM-MSCs was reported.²³ Thus, we wondered whether it was also elevated in MM cell lines exposed to MM-MSCs' ECM. CXCR4 expression levels were quantified in MM cell lines exposed to BM-MSCs' ECM (ND, MM) for 24 hours and a significant increase in the receptor expression (160%, $P < 0.05$) was induced by MM-MSCs' ECM but not ND-MSCs' ECM (Fig 3, D).

Since we have previously shown that autophagy facilitates MM cells migration,¹⁶ we wanted to test its involvement in the MM-MSCs' ECM promotion of cell migration as well. Thus, we repeated the transwell experiments of MM cells exposed to control or MM-MSCs' ECM with or without 3MA. Indeed, 3MA completely abrogated the effect of the MM-MSCs' ECM on MM cells migration ($\downarrow 60\%$ – 120% , $P < 0.01$; Fig 4, A). These results indicate that MM cells exposed to MM-MSCs' ECM are capable of migration and invasion in an autophagy-dependent manner. The acquisition of these traits facilitates the MM malignant cells' spreading in the tissue and consequently disease progression.

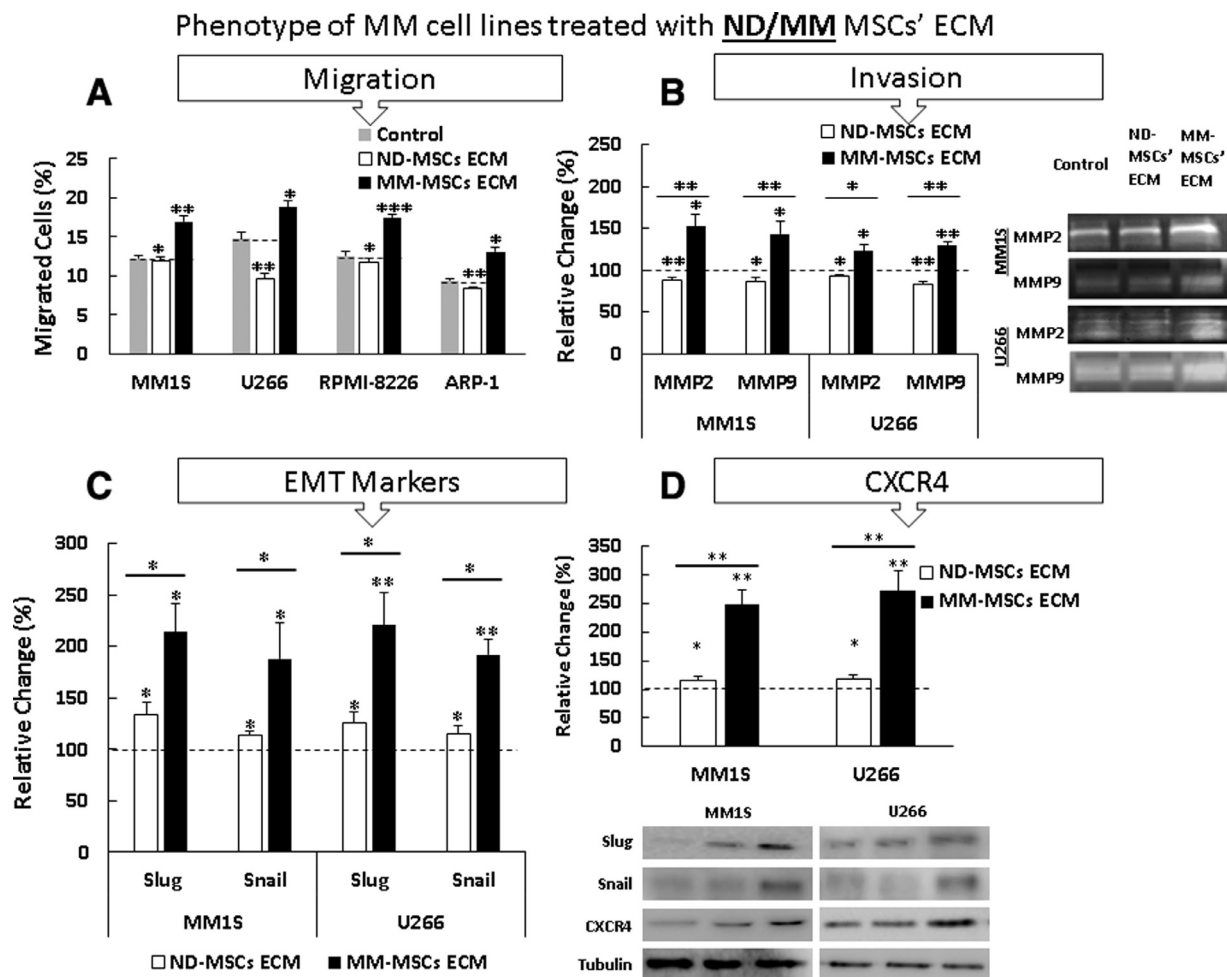


Fig 3. BM-MSCs' ECM effect on MM cell lines' phenotype MM cell lines (MM1S, U266, RPMI-8226, ARP-1) were cultured for 16 hours on BM-MSCs' ECM (ND, MM, and its own for control) and assayed for migration (A) (transwell), MMP9/MMP2 levels (B) (zymogram). Next, EMT markers (slug and Snail) were quantified after 24 hours culture on BM-MSCs' ECM (C). Finally, CXCR4 was extracted and quantified after the exposure to the BM-MSCs' ECM (D). Results are expressed as percent (Mean \pm SE, $n \geq 4$) of respective change. Asterisks depict statistical significance ($*P < 0.05$, $**P < 0.01$, $***P < 0.001$).

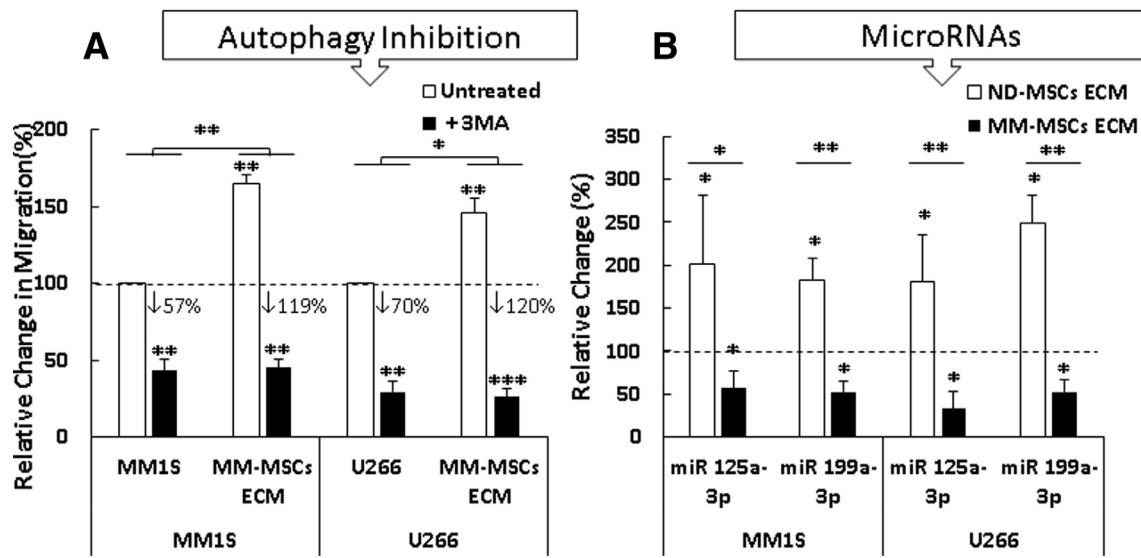
Phenotype of MM cell lines treated with ND/MM MSCs' ECM

Fig 4. BM-MSCs' ECM effect on MM cell lines' phenotype and microRNA expression. MM cell lines (MM1S, U266, RPMI-8226, ARP-1) were cultured for 16 hours on BM-MSCs ECM (ND, MM, and its own for control) in the presence of autophagy inhibitor 3MA, and then assayed for migration (A). Next, microRNAs were extracted, MIR-125a-3p and MIR-199a-3p expression levels were tested by qPCR (B). Results are expressed as percent (Mean \pm SE, $n \geq 4$) of respective change. Asterisks depict statistical significance (* $P < 0.05$, ** $P < 0.01$).

In a previous study, we have shown that altered expression of miR 125a-3p and miR 199a-3p microRNAs accompanied elevated MM cells migration.¹⁵ Thus, we tested their expression in our current research model as well (16 hours contact with ECM). Indeed, we determined significantly decreased/increased expressions in MM cells cultured on MM/ND-MSCs' ECM, respectively ($\downarrow 45\%$ – 70% and $\uparrow 80\%$ – 150% , respectively; $P < 0.05$; Fig 4, B).

The signaling of MM cell lines is affected by BM-MSCs ECM in a source-dependent manner. Based on our previous observations that MM cells' phenotype is often determined by MAPKs/TI signaling, we decided to examine these cascades in our experimental model.^{13,24}

MAPKs. First, we assayed the activation of ERK and JNK in MM cell lines exposed to their own respective ECM, ND-MSCs' ECM, and MM-MSCs' ECM in a time-dependent manner (15 minutes, 1, 4 and 24 hours; immunoblotting; Fig. 5 and 6). Results demonstrated that while MM-MSCs' ECM caused phosphorylation of JNK and ERK ($\uparrow 10\%$ – 40% , $P < 0.05$), ND-MSCs' ECM did not ($\downarrow 5\%$ – 20% , $P < 0.05$; Fig 5, A).

TI. Having established that MAPKs are activated in MM cells within the first hours of exposure to MM-MSCs ECM, we decided to examine TI factors previously shown to be their targets and involved in cell phenotype design.^{18,25,26} Indeed, we observed increased expression of pEIF4E and pEIF4GI in MM-MSCs ECM-treated MM cell lines (MM1S, U266, RPMI-8226, and ARP1) after 15 minutes, 1 hour, 4 hours, and 24 hours ($\uparrow 30\%$ – 70% , $P < 0.05$; Fig 5, B). In concordance with the downregulation of MM cells' JNK and ERK by ND-MSCs ECM, we also registered reduced phosphorylated TI factors in the malignant cells ($\downarrow 15\%$, $P < 0.05$; Fig 5, B). Inspection of a more extended response showed increased total and phosphorylated eIF4E and eIF4GI after 48–72 hours with MM-MSCs ECM ($\uparrow 25\%$ – 135% , $P < 0.05$); elevated TI factors' regulators (48–72

hours; $\uparrow 30\%$ – 200% , $P < 0.05$; Fig. 5, C and D, and 6); and targets (72 hours) ($\uparrow 30\%$ – 150% , $P < 0.05$; Fig 6). A reduction in TI factors/regulators/targets was observed in MM cell lines seeded on ND-MSCs ECM ($\downarrow 10\%$ – 55% , $P < 0.05$; Fig 6).

In order to validate that indeed the elevated MAPKs are responsible for the increased TI factors in our research model, we inhibited JNK (SP600125) and ERK (U0126) in MM-MSCs' ECM-treated MM cell lines (MM1S, U266). Then we reassayed the expression levels of pEIF4E and pEIF4GI in protein lysates of the MM cells. As expected, we observed that when JNK or ERK was inhibited, the MM-MSCs' ECM failed to promote the phosphorylation of TI factors in MM cell lines ($P < 0.05$; Fig 7, A and B).

Finally, we assayed the importance of active TI factors to the MM-MSCs' ECM-increased proliferation and migration by using the eIF4E-eIF4GI complex inhibitor 4EGI. Our observations demonstrated that 4EGI completely abolished the MM-MSCs ECM-induced migration ($P < 0.001$). Moreover, eIF4E-eIF4GI inhibition diminished the MM-MSCs ECM-induced proliferation of MM cells ($P < 0.001$; Fig 7, C). These results comply with our previous observations^{13,14,16} and once again demonstrate the dependence of MM cells' phenotype on TI. Taken together, we suggest that the MM-MSCs' ECM induces the signaling cascade of MAPKs/TI/phenotype in adjacent MM cells.

MM-MSCs ECM promotes MM cells' drug resistance. Our results so far indicated that MM-MSCs' ECM activated pathways with established roles in MM survival and drug resistance in the MM cells.²⁷ Specifically, we registered elevated MAPKs, NF κ B, HIF1 α , and autophagy ($\uparrow 30\%$ – 160% , $P < 0.05$; Fig. 2, E, 5, A, and 6). Thus, we tested the MM cells' (MM1S, U266) response to MM-MSCs ECM ($n = 3$) in the presence and absence of anti-MM drugs, that is, doxorubicin (Dox) and velcade (Vel). The drugs' dosages were determined by us

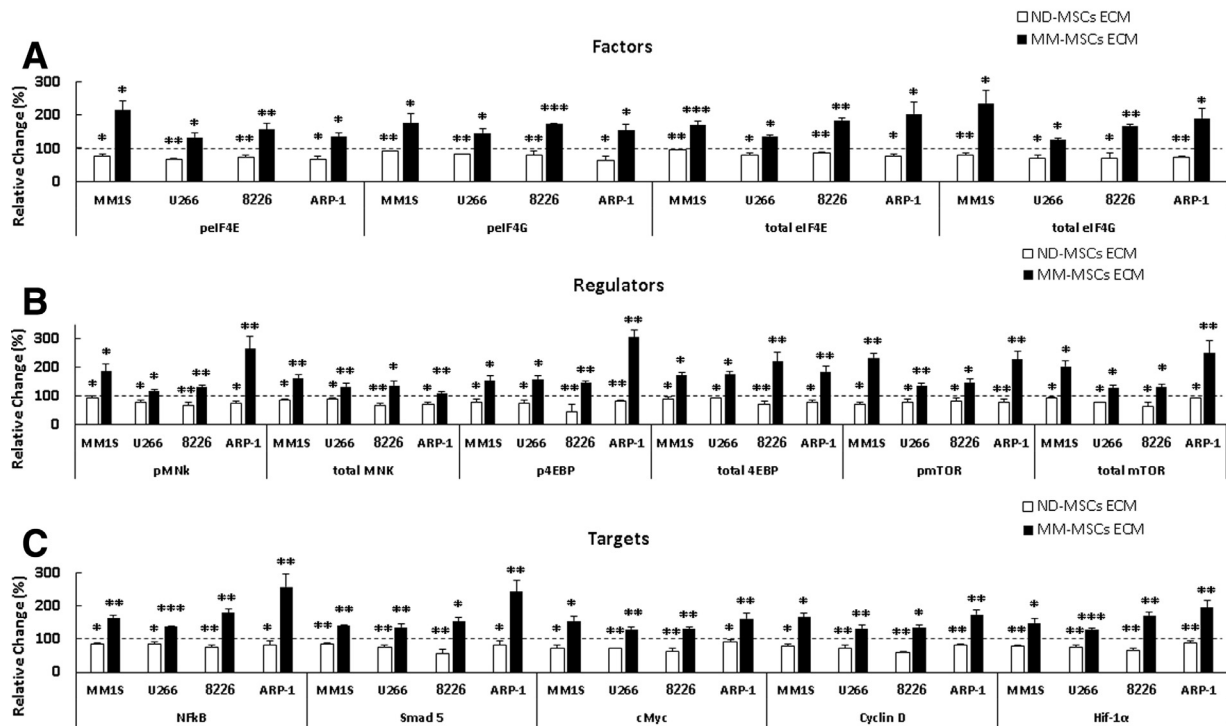
Signaling timeline of MM cell lines cultured on ND/MM MSCs' ECM

Fig 6. BM-MSCs' ECM effect on MM cells' MAPKs signaling and TI. MM cell lines (MM1S, U266, RPMI-8226, ARP-1) were cultured on 3 days BM-MSCs ECM (ND, MM, and its own for control) for 72 hours, lysed, and immunoblotted for (A) TI factors, (B) regulators, and (C) targets. Graphical presentation of analysis and representative immunoblots (supplementary Fig 1) are presented. Results are expressed as percent (Mean \pm SE, $n \geq 4$). Asterisks depict statistical significance (* $P < 0.05$, ** $P < 0.01$, *** $P < 0.001$).

This work is a continuance of our previous research that showed coculture of BM-MSCs with MM cells modulates the malignant cells' phenotype in accordance with the MSCs origin (ie, ND or MM).¹³ In an effort to isolate central mechanisms/pathways underlying this cooperation, we dissected the coculture model into solubles, MVs, and ECM. The contribution of the MM-MSCs' secretome and MVs to MM niche design and progression was demonstrated.^{14,16} Of note, the strength and significance of the secretome and MVs participation may stem from their systemic and far reaching influences. In the current study, we addressed the role of the BM-MSCs' ECM that is local and much less understood.

In a methodical study conducted by Jakubikova et al, the authors have compared 2D and 3D BM-MSCs' models and have shown that both models promote MM cells' proliferation.²³ Despite the authors' analyses of model fractions such as secreted cytokines or ECM components, the model was an all-inclusive coculture. Our aim was to characterize the mechanisms underlying our initial observations in the coculture model, yet we wanted to isolate the unique and independent effects of the different components in the coculture.^{13,16} Concordantly, in

this study, we elected to use a 2D 3 days ECM only model that is easier to produce, consistent, reliable, and specifically appropriate for the assays we conducted.²³ Finally, our choice to assay the ECM's contribution to Dox and Vel resistance was based on their relevance to MM therapy and published results of Jakubikova's group, which found that the added benefit of the 3D model to drug resistance was contingent on the drug: response to Dox independent of 2D/3D model and Vel dependent. In our study, there were no significant differences between the MM cell lines response to Dox and Vel. In summary, by using the reproducible 2D model, we were able to assay the response of MM cell lines to numerous BM-MSCs' ECM samples and reach new definite conclusions regarding the different roles of BM-MSCs ECM from normal and MM niches.

Autophagy is a cellular mechanism for maintaining homeostasis.¹¹ While its role in starvation and cellular stress is well established, more recent evidence demonstrates that autophagy may be induced upon loss of integrin-mediated cell attachments to surrounding ECM, thereby lending protection from anoikis.¹¹ Our results also show that the BM-MSCs ECM is capable of stimulating the MM cells' autophagy. Interestingly,

ND/MM MSCs' ECM affect MM cells phenotype via activation of MAPKs/TI cascade

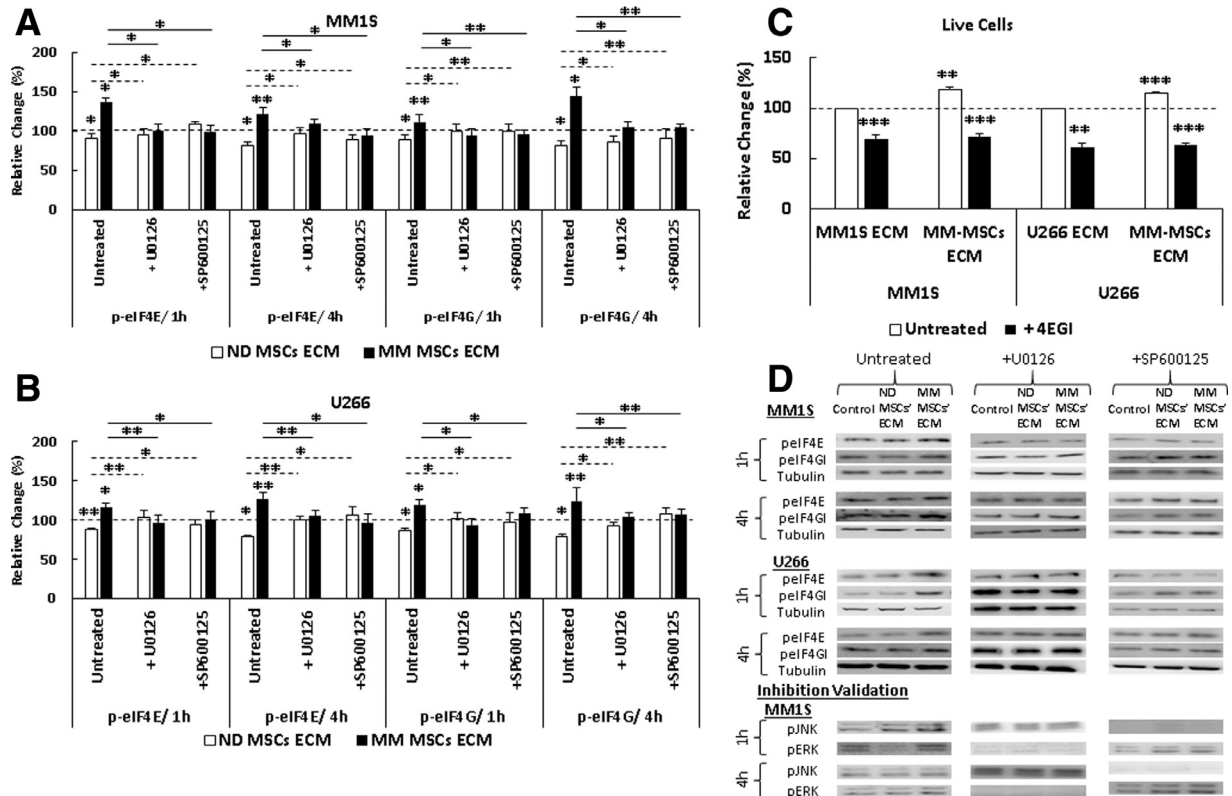


Fig 7. ND/MM MSCs' ECM affects MM cells phenotype via activation of MAPKs/TI cascade. MM1S and U266 cell lines were pretreated with MAPKs inhibitors (JNKi: SP600125 20 μ M; ERKi: U0126 10 μ M) for 1.5 hours, then cultured for 1 hour and 4 hours on 3 days BM-MSCs ECM (ND, MM, and its own for control). Cells were harvested, lysed, and immunoblotted for TI factors phosphorylation (A + B). Tubulin served as loading control. Next, MM cells were treated with eIF4E/eIF4G complex inhibitor 4EGI for 1 hour and then cultured with MM-MSCs' ECM then cell number were enumerated (C). Results are presented in graphs and representative immunoblots (D) and expressed as percent (Mean \pm SE, $n \geq 4$) of respective protein expression in control cells cultured on its own ECM (dotted line). Asterisks depict statistical significance (* $P < 0.05$, ** $P < 0.01$, *** $P < 0.001$).

we observed distinct differences in response intensities; MM cell lines exposed to MM-MSCs' ECM had higher amplifications of autophagy, while MM cells treated with ND-MSCs' ECM displayed the same trend but on a smaller scale. Several pathways regulate autophagy²⁹ and some were altered in our model of MM cells exposed to BM-MSCs' ECM (mTOR, NF κ B, MAPKs). Indeed, we propose that differences in the activation levels of these regulatory signals may explain the variation in autophagy levels. The role of CXCR4 in induction of autophagy and metastasis and its function at the interface of cells and their surroundings also piqued our interest. Indeed, MM cells have been previously shown to express CXCR4 and this has been linked to the BM homing, engraftment, and growth of the clonal plasma cells.³⁰ A recent study described CXCR4's contribution to acute myeloid leukemia cells' survival and autophagy.³¹ In accordance

with these reports, we also witnessed elevated CXCR4 levels in MM cell lines 24 hours after the exposure to BM-MSCs ECM, particularly from MM patients. Last, we demonstrated increased expression of EMT markers/transcription factors in the MM-MSCs' ECM-treated MM cells, an observation that supports the shift in MM cells' phenotype. Taken together, our observations substantiate a wide and encompassing influence to the ECM in MM design and the important participation of the MM-MSCs in MM support and progression.

In a review of MSCs' evolution in cancer, Cammarota and Laukkanen have summarized several reports on the differences in MSCs support of cancer in accordance to their normal or pathological origins.³² In concordance with our observations, they describe a cancer suppressing role for ND-MSCs and a cancer promoting effect attributed to MSCs from malignant settings. This influence is primarily ascribed to cell-cell contact.³²

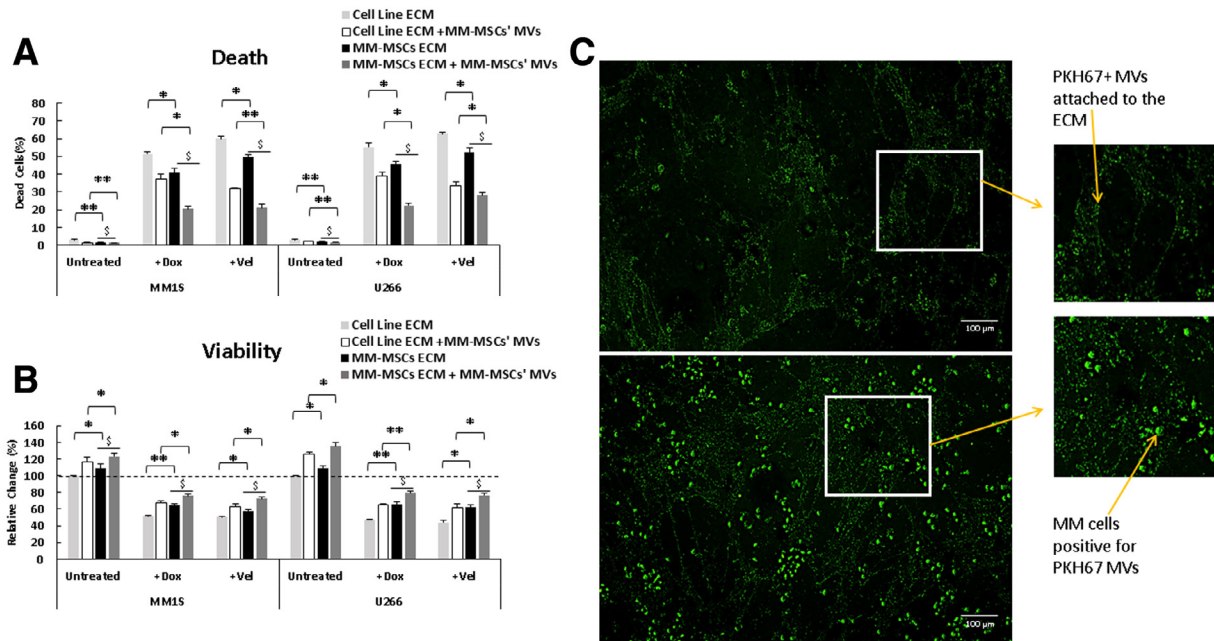
Drug Resistance of MM cell lines cultured on ND/MM MSCs' ECM

Fig 8. BM-MSCs' ECM effect on MM cells drug resistance. MM1S and U266 MM cell lines were cocultured with MM-MSCs ECM (3 days), MM-MSCs' MVs (50 ng) and anti-MM drugs (0.5 μ M doxorubicin, 1 nM velcade). Respective MM cells lines' ECM served as control. The cells were cultured on the ECM for 24 hours with or without the added MM-MSCs MVs and then supplemented with the respective drugs for another 24 hours. Harvested MM cells were assessed for cell death (A) (trypan blue) and viability (B) (WST1). Results are expressed as percent of respective MM cells cultured on their own ECM only (Mean \pm SE, $n \geq 4$) (dotted line). Asterisks depict statistical significance (\$ additive, * $P < 0.05$, ** $P < 0.01$). Panel (C top) exhibits a representative picture of 3 days' MM-MSCs' ECM with attached PKH67 dyed MM-MSCs MVs (after rinsing with PBS; depicted by arrow). Panel (C bottom) presents the situation after 24 hours where MM cells layered on the ECM + MVs have internalized the fluorescent MVs and are fluorescent as well (depicted by arrow).

Our results demonstrate the integral role of BM-MSCs' ECM in the communication between the malignant MM cells and their surroundings. The significance of ECM to cancer development, progression, and drug resistance is not novel.¹¹ It is also recognized that the ECM is highly plastic, ever-changing, and capable of affecting adjacent cells via multiple mechanisms (stiffness, composition, and various bound factors). Our results expand current knowledge by showing that the transformation of ND-MSCs into MM-MSCs is also reflected in their secreted ECM, which critically modulates the MM cells phenotype.

Overcoming CAM-DR is a well-recognized objective in MM.¹¹ Concordantly, the composition of ECM to CAM-DR is also acknowledged.¹¹ Cellular binding of ECM is often executed by integrins and activates survival pathways such as NF κ B.³³ Indeed, we also witnessed activation of signals known to promote MM cells survival and drug resistance. The microenvironment plays a central role in the malignant cells capability to reversibly change signal transduction or gene expression programs.³³ The discovery of EVs has

revealed a new and exciting means to achieve this plasticity without genetic change/mutations to the cells.^{2,33} Moreover, the systemic nature of the vesicles enables them to modify both cancer cells and stroma. Indeed, it was reported that EVs can bind ECM and promote wound-healing processes and affect cell proliferation, survival, and migration.³⁴ Accordingly, EVs are also implicated in drug resistance, MVs included.^{2,35} Here, we expanded on these data and demonstrated the cooperation between MM-MSCs-secreted ECM and associated MVs in cancer promotion, for example, drug response. Specifically, we showed that the secreted MM-MSCs' MVs can bind to the ECM, internalize the ECM-associated MM cells, and increase resistance in the recipient cells to anti-MM therapy. These observations underscore the need to further characterize the differences in ECM composition and MVs cargo of ND-MSCs and MM-MSCs in order to identify novel therapeutic targets.

The undervalued field of ECM biology is attracting more attention of late and is yielding novel findings that promote our understanding of the ECM's origins,

composition, and mechanisms of action. This data is expected to eventually allow us to develop ways to manipulate ECM to our advantage. New models are being developed to enable in vitro study of select tumor microenvironment (TME) components and cutting edge methods of analysis are employed for advanced characterization.^{2,36} Indeed, the MM ECM matrisome was recently analyzed and results demonstrated distinct differences that correlate with disease stage and patient survival.² Concordantly, our results demonstrate that the ECM of MSCs present in the BM niche is sufficient to affect the MM cells' phenotype. This is hardly surprising since like fibroblasts the MSCs are a major source for ECM.^{37,38} When the BM-MSCs' ECM is combined with additional TME components, in our case MVs, the effects are even greater. Moreover, the ECM is capable of retaining by association the MVs²⁸ (data not shown) thereby compiling their local effects. These novel data exacerbate the complexity and importance of the ECM bioscaffold to MM and underscore the need for additional studies in order to identify targetable signals essential to MM progression and drug resistance.

ACKNOWLEDGMENTS

Conflicts of Interest: All authors have read the journal's authorship agreement and the manuscript has been reviewed by and approved by all named authors. There is no conflict of interest.

This work was supported by the Cancer Biology Research Center (CBRC) #0601242482 Djerassi-Elias Dream Idea Grant, Tel Aviv University.

Author contributions are as follows: A. Ibraheem conceived, carried out experiments, and analyzed data; O. Jarchowsky collected MM patients for the study; O. Attar-Schneider, M. Dabbah, and S. Tartakover Matalon advised on experimental design and data analysis; L. Drucker and M. Lishner conceived experiments analyzed data and wrote paper.

The study was performed in partial fulfillment of the requirements for M.Sc. degree of Amjd Ibraheem, Sackler Faculty of Medicine, Tel Aviv University, Tel Aviv, Israel. The authors are grateful to the staff of the Hematocytological Laboratory at Meir Medical Center, Kfar Saba, Israel for its dedicated technical support.

SUPPLEMENTARY MATERIALS

Supplementary material associated with this article can be found in the online version at [doi:10.1016/j.trsl.2019.01.003](https://doi.org/10.1016/j.trsl.2019.01.003).

REFERENCES

1. Hynes RO. The extracellular matrix: not just pretty fibrils. *Science* 2009;326:1216–9.
2. Glavey SV, Naba A, Manier S, et al. Proteomic characterization of human multiple myeloma bone marrow extracellular matrix. *Leukemia* 2017;31:2426–34.
3. Bordeleau F, Chan B, Antonyak MA, et al. Microvesicles released from tumor cells disrupt epithelial cell morphology and contractility. *J Biomech* 2016;49:1272–9.
4. Lu P, Takai K, Weaver VM, et al. Extracellular matrix degradation and remodeling in development and disease. *Cold Spring Harb Perspect Biol* 2011;3:doi: 10.1101/cshperspect.a005058.
5. Marinkovic M, Block TJ, Rakian R, et al. One size does not fit all: developing a cell-specific niche for in vitro study of cell behavior. *Matrix Biol* 2016;52-54:426–41.
6. Geiger B, Spatz JP, Bershadsky AD. Environmental sensing through focal adhesions. *Nat Rev Mol Cell Biol* 2009;10:21–33.
7. Seetharaman S, Etienne-Manneville S. Integrin diversity brings specificity in mechanotransduction. *Biol Cell* 2018;110:49–64.
8. Slany A, Haudek-Prinz V, Meshcheryakova A, et al. Extracellular matrix remodeling by bone marrow fibroblast-like cells correlates with disease progression in multiple myeloma. *J Proteome Res* 2014;13:844–54.
9. Manier S, Sacco A, Leleu X, et al. Bone marrow microenvironment in multiple myeloma progression. *J Biomed Biotechnol* 2012;2012:157496.
10. Garcia-Gomez A, De Las Rivas J, Ocio EM, et al. Transcriptional profile induced in bone marrow mesenchymal stromal cells after interaction with multiple myeloma cells: implications in myeloma progression and myeloma bone disease. *Oncotarget* 2014;5:8284–305.
11. Di Marzo L, Desantis V, Solimando AG, et al. Microenvironment drug resistance in multiple myeloma: emerging new players. *Oncotarget* 2016;7:60698–711.
12. Kawano Y, Roccaro AM, Ghobrial IM, et al. Multiple myeloma and the immune microenvironment. *Curr Cancer Drug Targets* 2017;17:806–18.
13. Attar-Schneider O, Zismanov V, Dabbah M, et al. Multiple myeloma and bone marrow mesenchymal stem cells' crosstalk: effect on translation initiation. *Mol Carcinog* 2016;55:1343–54.
14. Dabbah M, Attar-Schneider O, Tartakover Matalon S, et al. Microvesicles derived from normal and multiple myeloma bone marrow mesenchymal stem cells differentially modulate myeloma cells' phenotype and translation initiation. *Carcinogenesis* 2017;38:708–16.
15. Dabbah M, Attar-Schneider O, Zismanov V, et al. Multiple myeloma cells promote migration of bone marrow mesenchymal stem cells by altering their translation initiation. *J Leukoc Biol* 2016;100:761–70.
16. Marcus H, Attar-Schneider O, Dabbah M, et al. Mesenchymal stem cells secretomes' affect multiple myeloma translation initiation. *Cell Signal* 2016;28:620–30.
17. Attar-Schneider O, Drucker L, Zismanov V, et al. Bevacizumab attenuates major signaling cascades and eIF4E translation initiation factor in multiple myeloma cells. *Lab Invest* 2012;92:178–90.
18. Attar-Schneider O, Zismanov V, Drucker L, et al. Secretome of human bone marrow mesenchymal stem cells: an emerging player in lung cancer progression and mechanisms of translation initiation. *Tumour Biol* 2016;37:4755–65.
19. Zismanov V, Attar-Schneider O, Lishner M, et al. Multiple myeloma proteostasis can be targeted via translation initiation factor eIF4E. *Int J Oncol* 2015;46:860–70.

20. Zhang H, Pang Y, Ma C, et al. CIC5 decreases the sensitivity of multiple myeloma cells to bortezomib via promoting pro-survival autophagy. *Oncol Res* 2017. <https://doi.org/10.3727/096504017X15049221237147>.
21. Ciobotaro P, Drucker L, Neumann A, et al. The effects of doxorubicin on apoptosis and adhesion molecules of normal peripheral blood leukocytes-an ex vivo study. *Anticancer Drugs* 2003;14:383–9.
22. Yagi H, Tan W, Dillenburg-Pilla P, et al. A synthetic biology approach reveals a CXCR4-G13-Rho signaling axis driving transendothelial migration of metastatic breast cancer cells. *Sci Signal* 2011;4:ra60.
23. Jakubikova J, Cholujova D, Hideshima T, et al. A novel 3D mesenchymal stem cell model of the multiple myeloma bone marrow niche: biologic and clinical applications. *Oncotarget* 2016;7:77326–41.
24. Attar-Schneider O, Pasmanik-Chor M, Tartakover-Matalon S, et al. eIF4E and eIF4G1 have distinct and differential imprints on multiple myeloma's proteome and signaling. *Oncotarget* 2015;6:4315–29.
25. Lau MT, So WK, Leung PC. Fibroblast growth factor 2 induces E-cadherin down-regulation via PI3K/Akt/mTOR and MAPK/ERK signaling in ovarian cancer cells. *PLoS One* 2013;8:e59083.
26. Shveygert M, Kaiser C, Bradrick SS, et al. Regulation of eukaryotic initiation factor 4E (eIF4E) phosphorylation by mitogen-activated protein kinase occurs through modulation of Mnk1-eIF4G interaction. *Mol Cell Biol* 2010;30:5160–7.
27. Dehghanifard A, Kaviani S, Abroun S, et al. Various signaling pathways in multiple myeloma cells and effects of treatment on these pathways. *Clin Lymphoma Myeloma Leuk* 2018;18:311–20.
28. Huleihel L, Hussey GS, Naranjo JD, et al. Matrix-bound nanovesicles within ECM bioscaffolds. *Sci Adv* 2016;2:e1600502.
29. Panda PK, Mukhopadhyay S, Das DN, et al. Mechanism of autophagic regulation in carcinogenesis and cancer therapeutics. *Semin Cell Dev Biol* 2015;39:43–55.
30. Alsayed Y, Ngo H, Runnels J, et al. Mechanisms of regulation of CXCR4/SDF-1 (CXCL12)-dependent migration and homing in multiple myeloma. *Blood* 2007;109:2708–17.
31. Hu X, Mei S, Meng W, et al. CXCR4-mediated signaling regulates autophagy and influences acute myeloid leukemia cell survival and drug resistance. *Cancer Lett* 2018;425:1–12.
32. Cammarota F, Laukkanen MO. Mesenchymal stem/stromal cells in stromal evolution and cancer progression. *Stem Cells Int* 2016;2016:4824573.
33. Davies AE, Albeck JG. Microenvironmental signals and biochemical information processing: cooperative determinants of intratumoral plasticity and heterogeneity. *Front Cell Dev Biol* 2018;6:44.
34. Rackov G, Garcia-Romero N, Esteban-Rubio S, et al. Vesicle-mediated control of cell function: the role of extracellular matrix and microenvironment. *Front Physiol* 2018;9:651.
35. Namee NM, O'Driscoll L. Extracellular vesicles and anti-cancer drug resistance. *Biochim Biophys Acta* 2018;1870(2):123–36.
36. Fairfield H, Falank C, Farrell M, et al. Development of a 3D bone marrow adipose tissue model. *Bone* 2018;BON-11541:1–12.
37. Pleyer L, Valent P, Greil R. Mesenchymal stem and progenitor cells in normal and dysplastic hematopoiesis-masters of survival and clonality? *Int J Mol Sci* 2016;17:1009.
38. Roson-Burgo B, Sanchez-Guijo F, Del Canizo C, et al. Insights into the human mesenchymal stromal/stem cell identity through integrative transcriptomic profiling. *BMC Genomics* 2016;17:944.